



**HAL**  
open science

## Investigation of Intrinsically Disordered Proteins through Exchange with Hyperpolarized Water

Dennis Kurzbach, Estel Canet, Andrea G. Flamm, Aditya Jhajharia,  
Emmanuelle M. M. Weber, Robert Konrat, Geoffrey Bodenhausen

► **To cite this version:**

Dennis Kurzbach, Estel Canet, Andrea G. Flamm, Aditya Jhajharia, Emmanuelle M. M. Weber, et al.. Investigation of Intrinsically Disordered Proteins through Exchange with Hyperpolarized Water. *Angewandte Chemie International Edition*, 2017, 56 (1), pp.389-392. 10.1002/anie.201608903 . hal-02017713

**HAL Id: hal-02017713**

<https://hal.sorbonne-universite.fr/hal-02017713v1>

Submitted on 13 Feb 2019

**HAL** is a multi-disciplinary open access archive for the deposit and dissemination of scientific research documents, whether they are published or not. The documents may come from teaching and research institutions in France or abroad, or from public or private research centers.

L'archive ouverte pluridisciplinaire **HAL**, est destinée au dépôt et à la diffusion de documents scientifiques de niveau recherche, publiés ou non, émanant des établissements d'enseignement et de recherche français ou étrangers, des laboratoires publics ou privés.

# Investigation of Intrinsically Disordered Proteins through Exchange with Hyperpolarized Water

Dennis Kurzbach,\* Estel Canet, Andrea G. Flamm, Aditya Jhajharia, Emmanuelle M. M. Weber, Robert Konrat, and Geoffrey Bodenhausen

**Abstract:** Hyperpolarized water can selectively enhance NMR signals of rapidly exchanging protons in osteopontin (OPN), a metastasis-associated intrinsically disordered protein (IDP), at near-physiological pH and temperature. The transfer of magnetization from hyperpolarized water is limited to solvent-exposed residues and therefore selectively enhances signals in  $^1\text{H}$ - $^{15}\text{N}$  correlation spectra. Binding to the polysaccharide heparin was found to induce the unfolding of preformed structural elements in OPN.

Intrinsically disordered proteins (IDPs) constitute a class of physiologically active proteins that lack stable secondary and tertiary structures.<sup>[1]</sup> The highly dynamic nature of these proteins endows them with an inherent ability to interact simultaneously with multiple binding partners in the cellular environment.<sup>[2]</sup> IDPs thus frequently constitute important hubs in protein interaction networks. The malfunction of IDPs often leads to severe diseases associated with deregulation of the cellular machinery.<sup>[3]</sup> Since intrinsically disordered proteins or regions constitute approximately 30% of the human proteome,<sup>[4]</sup> understanding their functionality and structure–function relationships is clearly desirable, especially with a view to developing novel therapeutic strategies for the treatment and prevention of diseases related to IDP malfunction.<sup>[5]</sup>

The inherent dynamics and flexibility of IDPs explain their astonishingly rich interactome. Nuclear magnetic resonance (NMR) spectroscopy has developed into a key method for the study of IDPs.<sup>[6]</sup> Multidimensional techniques and high-field NMR spectrometers give access to residue-resolved dynamics of IDPs at ambient temperature and low pH.<sup>[7]</sup> However, under physiological conditions, the spectra typi-

cally suffer from strong signal overlap and broadening, thus leading to peak intensities below the detection threshold.<sup>[8]</sup> To the best of our knowledge, only one study has been published so far that employs  $^1\text{H}$ - $^{15}\text{N}$  correlation spectra of IDPs under physiological conditions at pH 7.4 and 37°C.<sup>[9]</sup>

These limitations in the study of IDPs can be overcome by using hyperpolarized HDO<sup>[10]</sup> produced through dissolution dynamic nuclear polarization (D-DNP).<sup>[11]</sup> Because exchange between hyperpolarized HDO and amide  $\text{H}^{\text{N}}$  protons only enhances a limited set of solvent-exposed residues under near-physiological conditions,<sup>[8]</sup> the  $^1\text{H}$ - $^{15}\text{N}$  correlation spectra are sparse and can be assigned despite the poor dispersion of their chemical shifts.<sup>[12]</sup> Such sparse spectra are reminiscent of “spectral dilution” techniques that rely on  $^{13}\text{C}$  labelling of selected amino acids.<sup>[13]</sup> Felli and co-workers have advocated the use of  $^{13}\text{C}$  direct detection techniques that allow the observation of IDPs under physiological conditions in  $^{13}\text{C}$ - $^{15}\text{N}$  correlation spectra but do not show any proton signals, which are the object of our work.<sup>[14]</sup>

Osteopontin (OPN, Figure 1 a) is a cancer- and metastasis-associated IDP that can interact with heparin, an analogue of the natural ligand hyaluronic acid (HA).<sup>[15]</sup> By using hyperpolarized HDO to selectively observe residues that undergo fast exchange with the solvent, it is possible to follow the structural and dynamical adaptations of OPN induced by binding to heparin at pH 7.4 and 37°C.

To hyperpolarize water, we employ dissolution DNP (D-DNP).<sup>[16]</sup> A volume of 100  $\mu\text{L}$  of a 20 mM solution of 4-hydroxy-2,2,6,6-tetramethylpiperidin-1-oxyl (TEMPO) in  $\text{H}_2\text{O}$ , mixed 1:1 (v/v) with glycerol as a glass-forming solvent, is frozen at 1.2 K in a magnetic field of 6.7 T. Microwave irradiation near 188.2 GHz on resonance with the paramagnetic centers leads to hyperpolarization  $P(^1\text{H}) = 89\%$  in the glassy solid.<sup>[10a]</sup> The 200  $\mu\text{L}$  hyperpolarized solid are rapidly dissolved by a burst of 5 mL (25-fold dilution) preheated  $\text{D}_2\text{O}$  (180°C, 10.5 bar) and transported in approximately 6 s through a magnetic tunnel to a suitably buffered protein solution that is waiting in a 5 mm NMR sample tube in a high-resolution 800 MHz NMR spectrometer. The protein solution was adjusted to pH 8 before dissolution, so that a near-physiological pH 7.5 is reached after dilution. The temperature of the sample was approximately 308 K (35°C) after mixing. Our approach is summarized in Figure 1 b.<sup>[17]</sup> The most exposed amide ( $\text{H}^{\text{N}}$ ) protons of the protein rapidly exchange with the hyperpolarized HDO (after 40-fold dilution of  $\text{H}_2\text{O}$  in  $\text{D}_2\text{O}$ , most solvent protons are found in the form of HDO), while non-exposed residues exchange slower. After a delay of 8 s to allow turbulence to settle, a band-selective optimized-flip-angle short-transient hetero-

[\*] Dr. D. Kurzbach, E. Canet, A. Jhajharia, E. M. M. Weber, Prof. G. Bodenhausen  
Département de Chimie, Ecole Normale Supérieure  
PSL Research University, UPMC Univ Paris 06  
CNRS, Laboratoire des Biomolécules (LBM)  
24 rue Lhomond, 75005 Paris (France)  
and  
Sorbonne Universités, UPMC Univ Paris 06  
Ecole Normale Supérieure, CNRS  
Laboratoire des Biomolécules (LBM), Paris (France)  
E-mail: kurzbach@ens.fr

A. G. Flamm, Prof. R. Konrat  
Department of Structural and Computational Biology  
Max F. Perutz Laboratories, University of Vienna  
Vienna BioCenter Campus 5, 1030 Vienna (Austria)

Supporting information for this article can be found under:  
<http://dx.doi.org/10.1002/anie.201608903>.

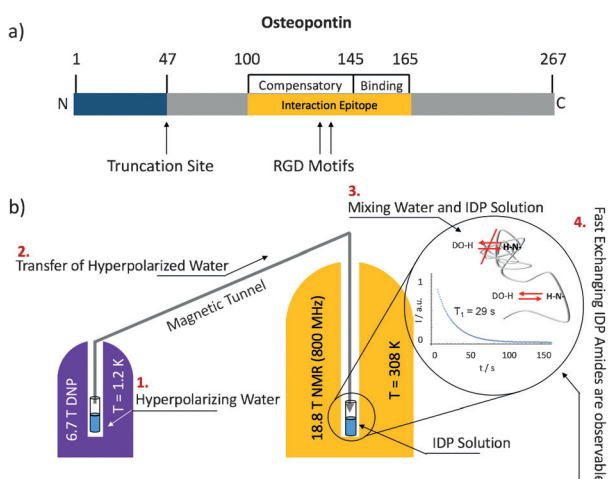


**Figure 1.** a) Sketch of the functional architecture of quail osteopontin (OPN). Full-length OPN consists of 267 amino acids. The metastasis-associated construct studied here comprises the 220 C-terminal residues (47–267) of the primary sequence. The heparin interaction epitope is located between residues 100 and 165. The heparin binding site comprises residues 145–165. The compensatory residues 100–145 become more mobile when bound to heparin. b) A mixture of H<sub>2</sub>O and glycerol containing 10 mM TEMPOL is hyperpolarized at 1.2 K and 6.7 T, dissolved with a 20-fold excess of superheated D<sub>2</sub>O, and transferred to an 18.8 T (800 MHz) spectrometer where it is mixed with a solution of OPN that is waiting in the NMR tube (ca. pH 7.5 and 308 K after mixing.) Strong signals in the <sup>1</sup>H-<sup>15</sup>N correlation spectra arise for rapidly exchanging protons (H<sup>N</sup>) in OPN, while slowly exchanging residues remain below the detection threshold.

nuclear multiple-quantum correlation (<sup>15</sup>N-<sup>1</sup>H SOFAST-HMQC) spectrum<sup>[18]</sup> was recorded in 19.2 s (see the Supporting Information).

Frydman and co-workers<sup>[19]</sup> have reported similar experiments, although their <sup>1</sup>H-<sup>15</sup>N correlation spectra do not feature any resolved resonances of individual amino acids that would be amenable to assignment. By contrast, we show that it is possible to monitor the folding and unfolding of individual residues of an IDP induced by the presence of ligands like heparin under near-physiological conditions. After dissolution, the TEMPOL concentration drops below 0.25 mM. The lifetime of the HDO proton hyperpolarization is  $T_1(^1\text{H}) = 29$  s, which is close to the value of HDO without TEMPOL.

The average relaxation time  $T_1(^1\text{H}^{\text{N}})$  of amide protons in OPN is on the order of 1 s,<sup>[20]</sup> but the proton polarization is replenished by exchange as long as the HDO (which is approximately in 100-fold excess with respect to the protein) remains hyperpolarized. The proton signals must be detected before the polarization becomes too weak.

Figure 2a shows a SOFAST-HMQC using hyperpolarized HDO (red) obtained in less than 30 s compared with a regular SOFAST-HMQC spectrum (black) of the same sample obtained in thermal equilibrium over 18 h. Note that the peaks of the regular SOFAST-HMQC are very broad, as expected at pH 7.5 and 35°C.<sup>[8]</sup> IDPs generally give rise to poorly dispersed peaks, and the signals are further broadened by fast proton exchange under our experimental conditions.<sup>[21]</sup>

Relaxation of the amide protons (H<sup>N</sup>) of OPN by TEMPOL is negligible.<sup>[22]</sup>

In the red hyperpolarized spectrum in Figure 2a, we only see enhanced signals for the most labile H<sup>N</sup> protons, which can exchange rapidly with HDO.<sup>[8]</sup> The exchange rates are estimated to be between 30–140 s<sup>-1</sup> at 35°C.

The probability that a hyperpolarized proton exchanges with OPN is at best 1/40 owing to the dilution of hyperpolarized protons with non-polarized protons and deuterons. Thus, for an exchange rate of 30 s<sup>-1</sup> and a recovery delay of 0.3 s (which was optimized empirically for our experiments), the probability to detect a hyperpolarized H<sup>N</sup> amide proton is only about 25%. This probability rises for exchange rates near 140 s<sup>-1</sup>. Thus, only rapidly exchanging protons have a sufficiently high probability to be detected, as displayed in Figure 2a.

Only residues that can exchange efficiently with the solvent on this time scale will be visible in our experiments, while residues that exchange more slowly will not be observed. The spectrum appears as if observed through a hyperpolarized exchange filter that suppresses <sup>1</sup>H-<sup>15</sup>N cross peaks for protons that slowly exchange with the solvent. Additionally, many peaks appear in the hyperpolarized SOFAST HMQC that cannot be observed through other methods owing to weak signal intensity at pH 7.5 and 35°C. Thus, exchange with the hyperpolarized HDO boosts the magnetization of fast exchanging residues above the detection limit.

In Figure 2b, an expansion of the serine and threonine region is shown. Our method not only has the advantage that the signals are amplified, but also that the enhancement is selective. The signals can therefore be assigned to their respective residues, which is not possible in a conventional 2D correlation spectrum because of extensive signal overlap (Figure 2b, black). Figure 2c shows the “bulk” signal of our hyperpolarized exchange filtered spectrum. Figure 2d and Figure S1 in the Supporting Information show overlays of OPN spectra, either enhanced by hyperpolarized HDO at pH 7.5 and 35°C, or detected in thermal equilibrium at pH 6.5 and 25°C, where the NMR signals are strongest in the absence of hyperpolarization.<sup>[15b]</sup> In high-resolution spectra obtained without hyperpolarization, many signals disappear when going from NMR-optimized to near-physiological conditions, that is, from pH 6.5 and 25°C to 7.5 and 35°C. These signals can be recovered through exchange with hyperpolarized water. Thus, a further advantage of our D-DNP technique is the observation of signals that are broadened beyond detection in conventional methods, although the resolution in hyperpolarized HMQC spectra suffers from rapid accumulation (< 30 s) after dissolution. Notwithstanding significant signal overlap, some peaks can still be assigned unambiguously. Even the N-terminal amino acids can be observed, which is normally impossible owing to fast solvent exchange. Here, however, for the very same reason, they become observable. Our method is therefore ideal for studying systems that cannot be studied otherwise owing to excessively fast exchange—a frequent obstacle is turned into an advantage in this method.

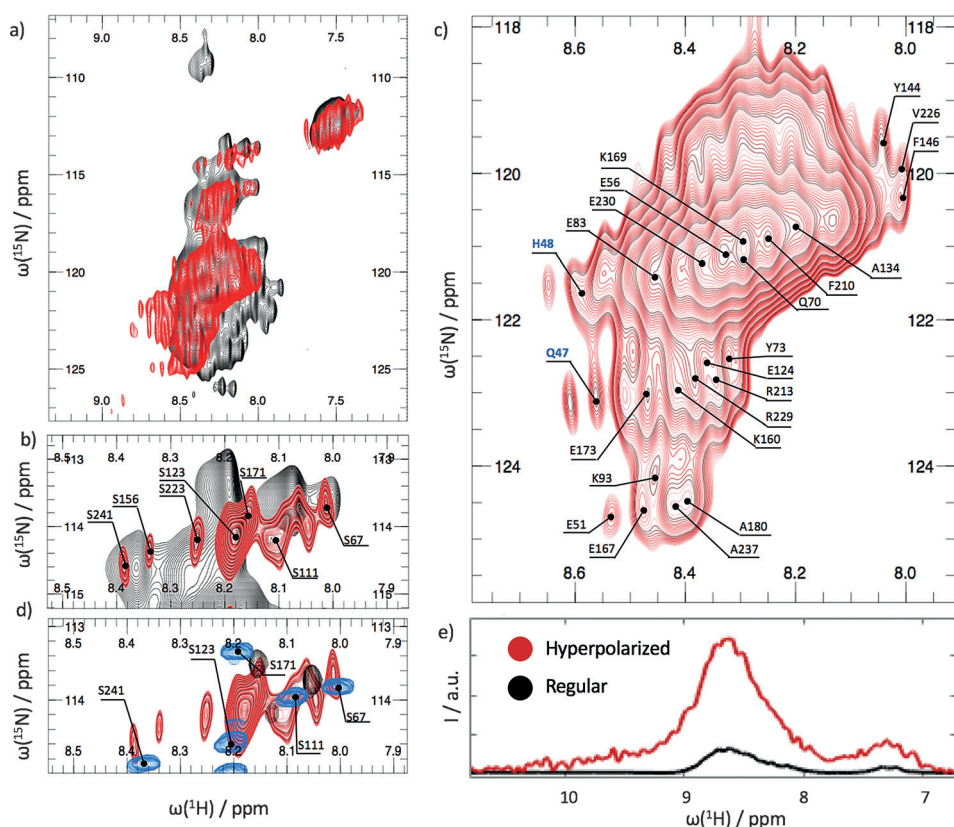


**Figure 2.** a) Red:  $^1\text{H}$ - $^{15}\text{N}$  correlation spectrum of OPN selectively enhanced by hyperpolarized HDO. Black: A regular spectrum of the same sample after return to thermal equilibrium. b) Region showing resonances of serines selectively enhanced by hyperpolarized HDO. c) The bulk signal still allows the assignment of some cross peaks. d) Overlay of a hyperpolarized exchange filtered SOFAST HMQC at pH 7.5 and 35°C (red), a high resolution HSQC with a recycling time of 1 s and 256 complex increments in the indirect dimension at pH 7.5 and 35°C (black), and the same HSQC with a recycling time of 1 s at pH 6.5 and 25°C (blue). Differences in chemical shifts between the red and the blue spectra stem from the different experimental conditions. For the overlay of the entire spectrum, see the Supporting Information. e) Comparison of the projection of the full  $^1\text{H}$ - $^{15}\text{N}$  spectra of OPN onto the proton dimension, detected with hyperpolarized water and SOFAST HMQC (red, see Figure 2c) in a single accumulation and the exact same experiment detected with 256 accumulations (black) after return to thermal equilibrium of the sample after dissolution. In both cases the recycling delay was set to 0.3 s. The two projections are scaled by the ratio of the number of spectra averaged (hyperpolarized/thermalized = 1:256) and the applied receiver gain (hyperpolarized/thermalized = 128:912). The signal enhancement due to hyperpolarized HDO was 40.

Note that the highest enhancement factors that were achieved for OPN were about 40 for the overall spectrum and 58 for the most intense peaks with respect to thermal equilibrium. Figure 2e shows a comparison between the signal intensities of OPN in a hyperpolarized exchange-filtered spectrum and a conventional spectrum in thermal equilibrium. Frydman and co-workers reported enhancement factors up to 330 at pH 7 and 60°C for denatured Trypsin (247 amino acids, like OPN). The enhancement factors should be compared with caution since the experimental conditions were quite different. Frydman and co-workers used a much faster injection system (1–3 s) and employed radical-separation techniques. Despite these differences, we may conclude that while we aim for physiological conditions that should be favorable for system-oriented studies, stronger signal enhancements may be obtained at other temperatures and pH. Furthermore, it has to be taken into account that in OPN,

the compacted core features reduced exchange rates so that many cross peaks are not enhanced by hyperpolarized HDO, while in entirely denatured proteins like that of Frydman and co-workers, all residues can be enhanced homogeneously.

In the complex of OPN bound to heparin, the binding site<sup>[15b,20]</sup> is located between residues 145–165 of OPN (Figure 1a). Between residues 100 and 145, a compensatory site is located that masks the binding site in the apo-state (i.e., in the absence of heparin), but is exposed to the solvent in the holo-state (i.e., when OPN is bound to heparin).<sup>[20]</sup> This feature, which compensates for entropy loss, is retained at near-physiological pH and temperature.

Figure 3a shows the Gly region of the hyperpolarized exchange filtered (red, 30 s) and normal (gray, obtained by time-averaging for 18 h) SOFAST HMQC spectra in the presence of heparin. Clearly, hyperpolarization allows the assignment of signals that are invisible in the normal spectrum owing to strong signal broadening. Most importantly, the glycine residues are not observable in the absence of heparin. Figure 3b shows how the  $\text{H}^{\text{N}}$  exchange rates are affected when heparin binds to OPN.

This leads to distinct effects in the glycine region. For exchange rates that increase upon binding, we observe that new cross-peaks emerge (green arrows in Figure 3d). In contrast, the only glycine that was observable in the apo-form becomes weaker owing to a decreased exchange rate in the holo-form (red arrow in Figure 3d). All visible glycine residues lie in the region between residues 100 and 180. They are more exposed to the solvent in the holo-form than in the apo-form.<sup>[20]</sup> This exposure accelerates exchange with hyperpolarized HDO, thereby rendering them amenable to detection. Only one glycine signal disappears upon heparin binding. It is located within the binding interface between residues 140–165, which display reduced exchange rates.

Figure 3c shows chemical-shift perturbations along the primary sequence of OPN observed by hyperpolarized exchange spectroscopy. These chemical shifts are in excellent agreement with earlier studies and highlight both the heparin

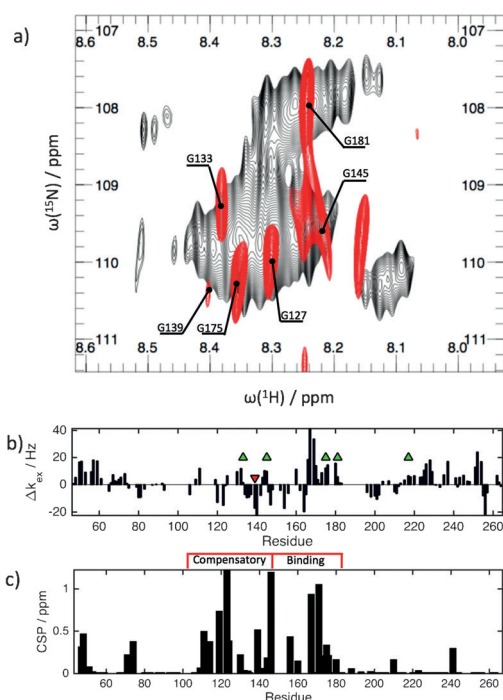


**Figure 3.** a) Expanded Ser/Thr region of the regular correlation spectrum of apo-OPN (partly folded in the absence of heparin; gray) and the spectrum of apo-OPN boosted by hyperpolarized HDO (colored). b) Differential exchange rates  $\Delta k_{\text{ex}} = k_{\text{ex}}(\text{holo}) - k_{\text{ex}}(\text{apo})$ . The green arrows indicate Gly residues that only appear in 2D correlation spectra of the holo-state of OPN. The red arrow indicates the only glycine resonance can be observed by means of hyperpolarized HDO in the apo-form. Its signal becomes weaker upon heparin binding. c) Chemical-shift perturbation (CSP) of resolved amino acid upon the binding of heparin to OPN.

binding site and the compensatory site.<sup>[20,23]</sup> Hyperpolarized HDO thus provides a reliable method to monitor conformational changes in IDPs.

## Acknowledgments

We thank Dr. Pavel Kadeřávek, Dr. Daniel Abergel, and Dr. Phillippe Pelupessy for their support, and Bruker BioSpin for generously providing the D-DNP prototype. This work was supported by the French CNRS, the European Research Council (ERC contract “Dilute para-water”), and the Austrian Science Foundation (FWF), P26317.

**Keywords:** dynamic nuclear polarization · hyperpolarized water · intrinsically disordered proteins · NMR spectroscopy · solvent exchange

**How to cite:** *Angew. Chem. Int. Ed.* **2017**, *56*, 389–392  
*Angew. Chem.* **2017**, *129*, 397–401

[1] a) P. Tompa, *Trends Biochem. Sci.* **2012**, *37*, 509–516; b) H. J. Dyson, P. E. Wright, *Nat. Rev. Mol. Cell Biol.* **2005**, *6*, 197–208; c) C. K. Fisher, C. M. Stultz, *Curr. Opin. Struct. Biol.* **2011**, *21*, 426–431.

- [2] M. Fuxreiter, P. Tompa, *Adv. Exp. Med. Biol.* **2012**, *725*, 1–14.  
 [3] M. M. Babu, R. van der Lee, N. S. de Groot, J. Gsponer, *Curr. Opin. Struct. Biol.* **2011**, *21*, 432–440.  
 [4] A. K. Dunker, Z. Obradovic, P. Romero, E. C. Garner, C. J. Brown, *Genome Inf. Ser.* **2000**, *11*, 161–171.  
 [5] L. Geist, M. A. Henen, S. Haiderer, T. C. Schwarz, D. Kurzbach, A. Zawadzka-Kazimierczuk, S. Saxena, S. Zerko, W. Kozminski, D. Hinderberger, R. Konrat, *Protein Sci.* **2013**, *22*, 1196–1205.  
 [6] a) T. Mittag, J. D. Forman-Kay, *Curr. Opin. Struct. Biol.* **2007**, *17*, 3–14; b) M. R. Jensen, M. Blackledge, *Proc. Natl. Acad. Sci. USA* **2014**, *111*, E1557–E1558.  
 [7] A. Zawadzka-Kazimierczuk, W. Kozminski, H. Sanderova, L. Krasny, *J. Biomol. NMR* **2012**, *52*, 329–337.  
 [8] G. S. Rule, T. K. Hitchens, *Fundamentals of Protein NMR Spectroscopy*, Springer, Dordrecht, **2006**.  
 [9] F. X. Theillet, A. Binolfi, B. Bekei, A. Martorana, H. M. Rose, M. Stuijver, S. Verzini, D. Lorenz, M. van Rossum, D. Goldfarb, P. Selenko, *Nature* **2016**, *530*, 45–50.  
 [10] a) Q. Chappuis, J. Milani, B. Vuichoud, A. Bornet, A. D. Gossert, G. Bodenhausen, S. Jannin, *J. Phys. Chem. Lett.* **2015**, *6*, 1674–1678; b) T. Harris, O. Szekely, L. Frydman, *J. Phys. Chem. B* **2014**, *118*, 3281–3290.  
 [11] A. Abragam, M. Goldman, *Rep. Prog. Phys.* **1978**, *41*, 395–467.  
 [12] G. Platzer, S. Zerko, S. Saxena, W. Kozminski, R. Konrat, *Biomol. NMR Assignments* **2015**, *9*, 289–292.  
 [13] a) V. Tugarinov, V. Kanelis, L. E. Kay, *Nat. Protoc.* **2006**, *1*, 749–754; b) J. Schörghuber, T. Sara, M. Bisaccia, W. Schmid, R. Konrat, R. J. Lichtenegger, *ChemBioChem* **2015**, *16*, 746–751.  
 [14] S. Gil, T. Hosek, Z. Solyom, R. Kummerle, B. Brutscher, R. Pierattelli, I. C. Felli, *Angew. Chem. Int. Ed.* **2013**, *52*, 11808–11812; *Angew. Chem.* **2013**, *125*, 12024–12028.  
 [15] a) D. Kurzbach, G. Platzer, T. C. Schwarz, M. A. Henen, R. Konrat, D. Hinderberger, *Biochemistry* **2013**, *52*, 5167–5175; b) G. Platzer, A. Schedlbauer, A. Chemelli, P. Ozdowy, N. Coudeville, R. Auer, G. Kontaxis, M. Hartl, A. J. Miles, B. A. Wallace, O. Glatter, K. Bister, R. Konrat, *Biochemistry* **2011**, *50*, 6113–6124; c) P. H. Anborgh, J. C. Mutrie, A. B. Tuck, A. F. Chambers, *J. Cell. Mol. Med.* **2010**, *14*, 2037–2044; d) L. R. Rodrigues, J. A. Teixeira, F. L. Schmitt, M. Paulsson, H. Lindmark-Mansson, *Cancer Epidemiol. Biomarkers* **2007**, *16*, 1087–1097; e) P. Y. Wai, P. C. Kuo, *J. Surg. Res.* **2004**, *121*, 228–241.  
 [16] J. H. Ardenkjaer-Larsen, B. Fridlund, A. Gram, G. Hansson, L. Hansson, M. H. Lerche, R. Servin, M. Thaning, K. Golman, *Proc. Natl. Acad. Sci. USA* **2003**, *100*, 10158–10163.  
 [17] a) D. Gajan, A. Bornet, B. Vuichoud, J. Milani, R. Melzi, H. A. von Kalker, L. Veyre, C. Thieuleux, M. P. Conley, W. R. Grüning, M. Schwarzwälder, A. Lesage, C. Copéret, G. Bodenhausen, L. Emsley, S. Jannin, *Proc. Natl. Acad. Sci. USA* **2014**, *111*, 14693–14697; b) B. Vuichoud, A. Bornet, F. de Nanteuil, J. Milani, E. Canet, X. Ji, P. Miéville, E. Weber, D. Kurzbach, A. Flamm, R. Konrat, A. D. Gossert, S. Jannin, G. Bodenhausen, *Chem. Eur. J.* **2016**, *22*, 14696.  
 [18] P. Schanda, E. Kupce, B. Brutscher, *J. Biomol. NMR* **2005**, *33*, 199–211.  
 [19] G. Olsen, E. Markhasin, O. Szekely, C. Bretschneider, L. Frydman, *J. Magn. Reson.* **2016**, *264*, 49–58.  
 [20] D. Kurzbach, T. C. Schwarz, G. Platzer, S. Höfler, D. Hinderberger, R. Konrat, *Angew. Chem. Int. Ed.* **2014**, *53*, 3840–3843; *Angew. Chem.* **2014**, *126*, 3919–3922.  
 [21] R. Konrat, *J. Magn. Reson.* **2014**, *241*, 74–85.  
 [22] G. M. Clore, J. Iwahara, *Chem. Rev.* **2009**, *109*, 4108–4139.  
 [23] a) D. Kurzbach, *Protein Sci.* **2016**, *25*, 1617–1627; b) D. Kurzbach, A. G. Flamm, T. Sara, *Protein Sci.* **2016**, *25*, 1628–1636.